Modeling of Shallow Quantum Point Contacts Defined on AlGaAs/GaAs Heterostructures: The Effect of Surface States

Gianluca Fiori
Dipartimento di Ingegneria dell'Informazione: Elettronica, Informatica, Telecomunicazioni, Università di Pisa
Giuseppe Iannaccone
Dipartimento di Ingegneria dell'Informazione: Elettronica, Informatica, Telecomunicazioni, Università di Pisa
Massimo Macucci
Dipartimento di Ingegneria dell'Informazione: Elettronica, Informatica, Telecomunicazioni, Università di Pisa

G. Fiori, G. Iannaccone, M. Macucci, "*Modeling of Shallow Quantum Point Contacts Defined on AlGaAs/GaAs Heterostructures: The Effect of Surface States*", Journal Computational Electronics, **1**, pp.39-42 (2002).

Journal of Computational Electronics 1: 39–42, 2002

Modeling of Shallow Quantum Point Contacts Defined on AlGaAs/GaAs Heterostructures: The Effect of Surface States

G. FIORI, G. IANNACCONE AND M. MACUCCI
Dipartimento di Ingegneria dell'Informazione, Università degli studi di Pisa, Via Diotisalvi 2, 56122, Pisa, Italy

Abstract. We have developed a program for the simulation of devices defined by electrostatic confinement on the two-dimensional electron gas in AlGaAs/GaAs heterostructures. Our code is based on the self-consistent solution of the Poisson-Schrödinger equation in three dimensions, and can take into account the effects of surface states at the semiconductor-air interface and of discrete impurities in the doped layer. We show results from the simulation of quantum point contacts with different lithographic gaps, whose conductance is computed by means of a code based on the recursive Green's functions formalism.

Keywords: heterostructures, mesoscopic devices, surface states

1. Introduction

The confining potential and the charge density in mesoscopic devices defined by electrostatic confinement in a shallow two-dimensional electron gas (2DEG) strongly depend on the properties of the surface, i.e., on the density of states and the semiconductor-air interface. For this reason, the accurate simulation of such devices requires that proper boundary conditions be enforced at the exposed semiconductor surface (Chen and Porod 1993, Davies and Larkin).

As shown in Iannaccone *et al.* (2000), the assumption of Fermi level pinning at the exposed surface, as well as the assumption of a constant electric field at the semiconductor-air interface, corresponding to a frozen surface charge, are not adequate to achieve results in quantitative agreement with experiments. In particular, for the case of quantum point contacts defined by split gates on an AlGaAs/GaAs heterostructure, these assumptions provide reasonably good results for small lithographic gaps, while for larger gaps do not even reproduce pinch-off of the channel, which is experimentally observed (Iannaccone *et al.* 2000).

A more detailed model of surface states must therefore be used: in particular, we use a model typical of metal-semiconductor contacts (Sze 1981), and based on two parameters: an "effective" work function Φ^* of the exposed surface, and a constant density of surface states per unit energy per unit area D_s. If E_0 is the energy of the vacuum level, we assume that surface states with energy lower than $E_0 - q\Phi^*$ behave as acceptor states, while surface states with energy higher than $E_0 - q\Phi^*$ behave as donor states.

2. Simulations

We have considered several quantum point contacts defined by split gates on an AlGaAs/GaAs heterostructure, with different lithographic gaps. The layer structure consists of an undoped GaAs substrate, an undoped 12 nm $Al_{0.2}Ga_{0.8}As$ spacer layer, a 31 nm layer of doped GaAs (approx. 10^{18} cm^{-3}) and an undoped 9 nm GaAs cap layer.

We have solved self-consistently the Schrödinger and Poisson equations in a three dimensional domain in order to obtain the profiles of the first subband and of the electron density in the 2DEG. The potential profile in the three-dimensional structure obeys the Poisson equation

$$\nabla[\varepsilon(\vec{r})\nabla\phi(\vec{r})] = -q[p(\vec{r}) - n(\vec{r}) + N_D^+(\vec{r}) - N_A^-(\vec{r})], \quad (1)$$

where ϕ is the electrostatic potential, ε is the dielectric constant, p and n are the hole and electron densities, respectively, N_D^+ is the concentration of ionized donors and N_A^- is the concentration of ionized acceptors. While hole, acceptor and donor densities are computed in the whole domain with the semiclassical approximation, the electron concentration in the 2DEG is computed by solving the Schrödinger equation with density functional theory.

The observation that electron confinement is strong along the direction perpendicular to the AlGaAs/GaAs interface has led us to decouple the Schrödinger equation into a 1D equation in the vertical (x) direction and a 2D equation in the y–z plane: the density of states in the horizontal plane is well approximated by the semiclassical expression, since there is no in-plane confinement, while discretized states appear in the vertical direction. The single particle Schrödinger equation in 3D reads

$$\begin{aligned} -\frac{\hbar^2}{2}\frac{\partial}{\partial x}\frac{1}{m_x}\frac{\partial}{\partial x}\Psi - \frac{\hbar^2}{2}\frac{\partial}{\partial y}\frac{1}{m_y}\frac{\partial}{\partial y}\Psi \\ -\frac{\hbar^2}{2}\frac{\partial}{\partial z}\frac{1}{m_z}\frac{\partial}{\partial z}\Psi + V\Psi = E\Psi; \end{aligned} \tag{2}$$

we can write $\Psi(x, y, z)$ as $\Psi(x, y, z) = \psi(x, y, z)\,\chi(y, z)$. By substituting the above expression in (2) we obtain the following expression

$$\begin{aligned} -\frac{\hbar^2}{2}\chi\frac{\partial}{\partial x}\frac{1}{m_x}\frac{\partial}{\partial x}\psi - \left[\frac{\hbar^2}{2}\frac{\partial}{\partial y}\frac{1}{m_y}\frac{\partial}{\partial y}\right. \\ \left. + \frac{\hbar^2}{2}\frac{\partial}{\partial z}\frac{1}{m_z}\frac{\partial}{\partial z}\right]\psi\chi + V\psi\chi = E\psi\chi, \end{aligned} \tag{3}$$

where the dependence on x, y and z is omitted for clarity. If ψ satisfies the Schrödinger equation along the x direction

$$-\frac{\hbar^2}{2}\frac{\partial}{\partial x}\frac{1}{m_x}\frac{\partial}{\partial x}\psi + V\psi = \tilde{E}(y, z)\,\psi, \tag{4}$$

by substituting (4) in (3) we obtain

$$\begin{aligned} -\left[\frac{\hbar^2}{2}\frac{\partial}{\partial y}\frac{1}{m_y}\frac{\partial}{\partial y} + \frac{\hbar^2}{2}\frac{\partial}{\partial z}\frac{1}{m_z}\frac{\partial}{\partial z}\right]\psi\chi \\ = E\psi\chi - \tilde{E}(y, z)\,\psi\chi. \end{aligned} \tag{5}$$

Assuming that $\psi(x, y, z)$ is weakly dependent on y and z, and defining

$$\hat{T}_{yz} \equiv -\frac{\hbar^2}{2}\frac{\partial}{\partial y}\frac{1}{m_y}\frac{\partial}{\partial y} - \frac{\hbar^2}{2}\frac{\partial}{\partial z}\frac{1}{m_z}\frac{\partial}{\partial z}, \tag{6}$$

(5) can be approximated as

$$\psi\hat{T}_{yz}\chi = \psi[E - \tilde{E}_i(y, z)]\,\chi, \tag{7}$$

where $\tilde{E}_i$ is the i-th eigenvalue of (4). Since $\tilde{E}_i(y, z)$ in the cases considered is rather smooth in y and z, we will assume that eigenvalues of (7) essentially obey the 2D semiclassical density of states.

The confining potential V can be written as $V = E_C + V_{exc}$, where E_C is the conduction band and V_{exc} is the exchange-correlation potential within the local density approximation (Inkson 1984).

$$V_{exc} = -\frac{q^2}{4\pi^2\varepsilon_0\varepsilon_r}[3\pi^3 n(\vec{r})]^{\frac{1}{3}} \tag{8}$$

For GaAs, we have $m_x = m_y = m_z = m = 0.067m_0$, where m_0 is the electron mass, therefore the electron density can be written as

$$\begin{aligned} n(x, y, z) = \frac{k_B T m}{\pi\hbar^2}\sum_{i=0}^{+\infty}|\psi_i(x, y, z)|^2 \\ \times \ln\left[1 + \exp\left(-\frac{\tilde{E}_i(y, z) - E_F}{k_B T}\right)\right] \end{aligned} \tag{9}$$

where ψ_i and $\tilde{E}_i$ are the eigenfunctions and eigenvalues of (4), respectively.

To solve self-consistently the Poisson-Schrödinger equation, we have used the Newton-Raphson method with a predictor/corrector algorithm close to that proposed in Trellakis *et al.* (1997). In particular, the Schrödinger equation is not solved at each Newton-Raphson iteration step. Indeed, if we consider the eigenfunction constant within a loop and eigenvalues shifted by a quantity $q(\phi - \tilde{\phi})$, where $\tilde{\phi}$ is the potential used in the previous solution of the Schrödinger equation and ϕ is the potential at the current iteration, then the electron density becomes

$$\begin{aligned} n(x, y, z) \\ = \frac{k_B T m}{\pi\hbar^2}\sum_i |\psi_i(x, y, z)|^2 \\ \times \ln\left[1 + \exp\left(-\frac{\tilde{E}_i(y, z) - E_F + q(\phi - \tilde{\phi})}{k_B T}\right)\right] \end{aligned} \tag{10}$$

The algorithm is then repeated cyclically until the norm of $\phi - \tilde{\phi}$ is smaller than a predetermined value.

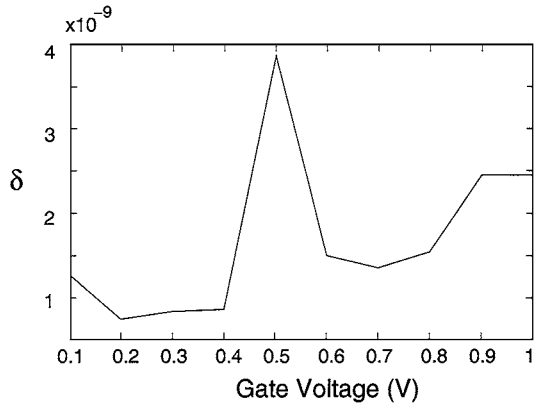

Figure 1. Plot of the parameter δ as a function of the gate voltage V_G for a quantum point contact with lithographic gap of 112 nm.

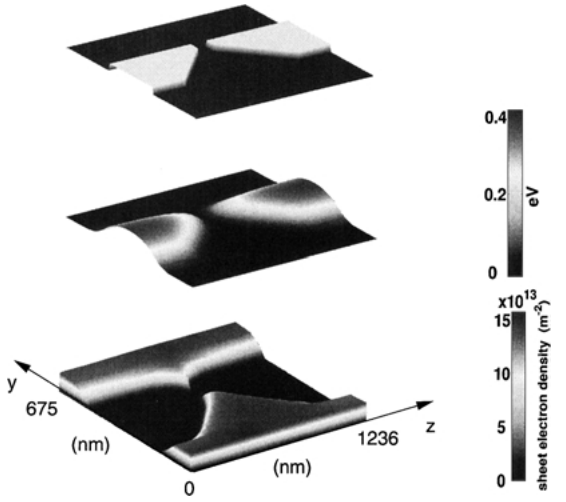

Figure 2. Gate layout of a quantum point contact with lithographic gap of 112 nm (top), theoretical first subband profile (center) and electron density in the 2DEG (bottom).

Once the subband profile is obtained, the conductance in the channel is computed with a method based on recursive Green's functions (Macucci, Galick and Ravaioli 1995).

2.1. *Decoupling of the Schrödinger Equation*

In order to assess the validity of the approximation which led us to decouple the Schrödinger equation, we define

$$a(x, y, z) \equiv \hat{T}_{yz}\psi_i\chi - \psi_i\hat{T}_{yz}\chi; \qquad (11)$$

$a(x, y, z)$ is the difference between the left-hand sides of (5) and (7), and, if the approximation is valid, must be much smaller than the right-hand side in any point of the domain. This means that the term δ, defined as

$$\delta \equiv \max_{x,y,z}\left|\frac{a(x, y, z)}{[E - \tilde{E}_i(y, z)]\,\phi\chi}\right|, \qquad (12)$$

must be much smaller than 1.

In Fig. 1 we plot δ as a function of the voltage applied on the split gates for a quantum point contact with lithographic gap of 112 nm. As can be seen, δ is smaller than 10^{-8} and therefore the approximation is very good.

3. Results

To reach convergence at the desired temperature of 4.2 K, a preventive "cooling" procedure is required, starting from 100 K, and progressively decreasing the temperature.

The parameters of the surface state model and the concentration of donors in the doped layer have been extracted from measurements on purposely fabricated test structures (Pala *et al.* submitted): $\Phi^* = 4.85$ eV, $D_S = 5 \times 10^{12}$ cm^{-2} eV^{-1}. N_D has been chosen as a fitting parameter in order to reproduce the experimental pinchoff voltages of QPCs with different lithographic gaps. The best fit is provided by $N_D = 0.8 \times 10^{18}$ cm^{-3}. The electron concentration in the 2DEG is 4×10^{11} cm^{-2}.

In Fig. 2 we plot the gate layout (above), the first subband in the 2DEG (center), and the electron density in the 2DEG (below) for a quantum point contact with lithographic gap of 112 nm and applied voltage of -0.5 V.

Theoretical G–V curves of QPCs with lithographic gap of 57, 112 and 140 nm are shown in Fig. 3. With just one fitting parameter (N_D), computed pinch-off voltages agree within 5% with the average experimental pinch-off voltages measured on the same structures (Fiori *et al.* submitted).

The concentration of impurities in the doped layer plays an important role in the electrical properties of devices realized on a 2DEG (Thean, Nagaraja and Leburton 1997). A simulation that takes into account the random distribution of impurities in the bulk is therefore necessary. In particular we assume that implanted impurities in the bulk obey a Poisson

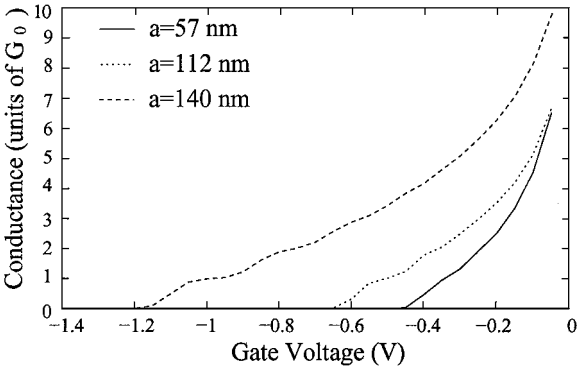

Figure 3. Simulated conductance as a function of gate voltage for devices with lithographic gaps of 57, 112, and 140 nm.

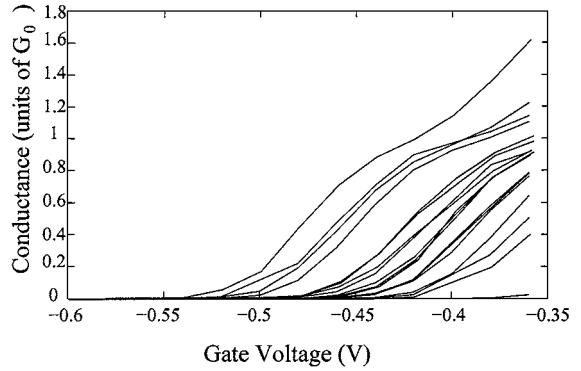

Figure 4. Simulated conductance as a function of gate voltage for 16 nominally identical quantum point contacts with $a = 57$ nm, but different actual discrete dopant density.

distribution. We have then simulated an ensemble of devices with identical nominal doping profile but different actual distribution of discrete impurities.

Simulated G–V curves of nominally identical quantum point contacts with different "actual" dopant distribution are shown in Fig. 4. For each point of the grid we have considered its associated element of volume ΔV and the nominal doping concentration N_D. The actual number of impurities in ΔV is obtained as a random number N' extracted with Poisson distribution of average $\Delta V \mathrm{N}_D$. Dividing N' by ΔV we obtain the actual local density of dopants.

We have obtained a standard deviation of the pinch-off voltage $\sigma_{N_D} = 41.5$ mV, which is about a half of the experimental value (Fiori *et al*. submitted). Such difference may be due to other sources of dispersion of the pinch-off voltage, such as geometric tolerances.

4. Conclusion

A solver of the Poisson-Schrödinger equations in three dimensions has been developed, which includes a model for surface states based on two parameters: an "effective" work function of the surface states and the density of surface states per unit area per unit energy. We have demonstrated that in the simulation of shallow QPCs the Schrödinger equation may be solved only in the vertical direction, with practically no loss of accuracy.

We have shown that our code can also include the effect of discrete impurities in the doped layer, and that such an effect accounts for about a half of the dispersion of pinch-off voltage measured in experiments.

Acknowledgment

Support from the NANOTCAD Project (IST-1999-10828 NANOTCAD) is gratefully acknowledged.

References

Chen M. and Porod W. 1993. J. Appl. Phys. 75: 2545.
Davies J.H. and Larkin I.A. 1994. Phys. Rev. B 49, 4800.
Fiori G., Iannaccone G., Macucci M., Reitzenstein S., Kaiser S., Kesselring M., Worschech L., and Forchel A. 2002. Nanotechnology 13: 299.
Iannaccone G., Macucci M., Amirante E., Jin Y., Lanois H., and Vieu C. 2000. Superlattices and Microstructures 27: 359.
Inkson J.C. 1984. Many Body Theory of Solids—An Introduction. Plenum, New York.
Macucci M., Galick A., and Ravaioli U. 1995. Phys. Rev. B 52: 5210.
Pala M., Iannaccone G., Kaiser S., Schliemann A., Worschech L., and Forchel A. 2002. Nanotechnology 13: 373.
Sze S. 1981. Physics of Semiconductor Devices, 2nd edn. Wiley and Sons, New York.
Thean V.Y., Nagaraja S., and Leburton J.P. 1997. J. Appl. Phys. 82: 1678.
Trellakis A., Galick A.T., Pacelli A., and Ravaioli U. 1997. J. Appl. Phys. 81: 7800.